model is written:

$$Y = b_0 + b_1X_1 + b_2X_2 + b_3X_1^2 + b_4X_1X_2 + b_5X_2^2 + \text{Error} \quad \text{(Eq. 1)}$$

where Y is the response surface such as tablet friability or drug dissolution, X_1 and X_2 are controllable variables such as granulation moisture and tablet crushing strength, and the coefficients b_0, b_1, ... b_5 are the least-square regression coefficients.

The results of the regression analysis are given in Table I. The regression coefficients were substituted in Eq. 1, and by fixing the moisture content, the calculated plots of tablet friability *versus* tablet crushing strength were obtained (Fig. 3). Similarly, by fixing the tablet crushing strength, calculated plots of tablet friability *versus* moisture content were obtained (Fig. 4). These plots suggest that the moisture content in the range of ~1.5–3.0% and tablet crushing strength in the range of ~14–17 Strong Cobb units (SCU) give the least possible tablet friability. Similar conclusions could be drawn from the data given in Fig. 1.

The response surface contour plots of friability and dissolution are given in Figs. 5 and 6. The response surface contour plots illustrate the geometric relationships between the controllable variables and their responses. The predicted values of responses for a grid of the controllable variable data points can be generated. The friability contour plot consists of a series of ellipsoidal curves. The solution for optimum response indicated that the predicted value of friability at optimum was 0.17%, corresponding to a moisture content of 2.3% and a tablet crushing strength of 16.8 SCU.

In tableting, tablet crushing strengths are generally limited to between 8 and 20 SCU because of compression, friability, and dissolution limitations. From Fig. 5 one can obtain a range of crushing strengths (14.2–19.4 SCU) and a range of moisture content (1.5–3%), which gives friability in the minimum possible range of 0.17–0.21%. At a fixed tablet crushing strength of 16 SCU, friability decreases as the moisture content increases until it reaches its optimum value. Further increase in moisture content results in an increase in friability. Similarly, at a fixed moisture content of 2%, friability decreases as the crushing strength is increased until an optimum value is reached, after which time material is generally incompressible due to the tablet density approaching the calculated true density of the formulation.

The response surface contour plots of dissolution given in Fig. 6 show a stationary ridge system. The stationary ridge system has parallel straight line contours running in a direction determined by the relative effect of X_1 and X_2, which are controllable variables. The response surface contour plots using Eq. 1 can take a number of different forms depending on the coefficients b_0, b_1, ... b_5.

Within the practical limitations of tableting, there are a large number of combinations of tablet crushing strength and granulation moisture content all along the ridge which is expected to give 100% drug dissolution. At constant crushing strength, an increase or decrease in the granulation moisture content moving away from the ridge in either direction results in lower dissolution. Similarly, at constant granulation moisture content, an increase or decrease in crushing strength moving away from the ridge results in lower drug dissolution.

In this investigation, not only *in vitro* dissolution but also tablet friability were considered important and both were measured experimentally. If it was desired that the specifications for dissolution in 10 min were >46% and to maintain friability <0.3%, Figs. 5 and 6 could be superimposed. The contour overlays are shown in Fig. 7. The shaded area shows the region where both the friability and dissolution requirements are met. From the deeply shaded rectangle, specifications on granulation moisture and tablet crushing strength could be set. If these specifications were unsatisfactory from a bioavailability or production viewpoint, other factors affecting friability and dissolution such as formulation and processing factors would have to be explored. It also may be possible to reduce tablet friability by considering the punch shape factor.

In conclusion, this study shows that a general multiple linear regression analysis is helpful in understanding the role of the granulation moisture and tablet crushing strength on tablet friability and *in vitro* dissolution. By superimposing the contour plots of tablet friability and drug dissolution, it is possible to set in process specifications for the granulation moisture content and tablet crushing strength.

REFERENCES

(1) Z. T. Chowhan and L. Palagyi, *J. Pharm. Sci.*, **67**, 1385 (1978).

(2) Z. T. Chowhan, *ibid.*, **69**, 1 (1980).

(3) Z. T. Chowhan, *Drug Dev. Ind. Pharm.*, **5**, 41 (1979).

(4) E. G. Shafer, E. G. Wollish, and C. E. Engel, *J. Am. Pharm. Assoc., Sci. Ed.*, **45**, 114 (1956).

(5) B. Selmeczi, *Sci. Pharm.*, **42**, 73 (1974).

(6) E. G. Wollish and A. R. Mlodzeniec, "Abstracts," APhA Academy of Pharmaceutical Sciences Annual Meeting, St. Louis, Mo., 94, vol. 11, No. 1 (1981).

Relationship of Dissolution Rate to Viscosity of Polymeric Solutions

NARONG SARISUTA * and EUGENE L. PARROTT ×

Received December 28, 1981, from the *Division of Pharmaceutics, College of Pharmacy, University of Iowa, Iowa City, IA 52242.* Accepted for publication February 5, 1982.

* Present address: Mahidol University, Bangkok, Thailand.

Abstract □ The influence of viscosity on the dissolution rate of benzoic acid in aqueous solutions of methylcellulose, hydroxypropyl cellulose, and guar gum was investigated. The viscosities were measured by capillary and rotational viscometers and were calculated from experimental diffusion coefficients by means of the Stokes-Einstein equation. The relationship of the dissolution rate to viscosity may be represented by a single curve. An equation is presented relating the dissolution rate of benzoic acid to solubility, diffusion coefficient, and viscosity for these nonionic viscosity-enhancing agents. To demonstrate that additional factors affect the dissolution rate, similar data were determined using solutions of xanthan gum, which is anionic. The electrical effect modified mass transport so the quantitative relationship of dissolution rate and viscosity was not the same as in the nonionic carbohydrate solution.

Keyphrases □ Dissolution, rate—relationship to viscosity of polymeric solutions, benzoic acid □ Viscosity—relationship of dissolution rate of polymeric solutions, benzoic acid □ Benzoic acid—relationship of dissolution rate to viscosity of polymeric solutions

Although viscosity-enhancing polymers are present in many pharmaceuticals, little research has been reported on the influence of viscosity on the dissolution rate. Diffusion-controlled dissolution would be expected to decrease in rate with an increase in viscosity (1–4). Numerous empirical equations, which show the dissolution rate to be a function of the viscosity raised to a power ranging from −0.25 to −0.8, have been proposed (5–7).

0022-3549/82/1200-1375$01.00/0

Table I—Solubility and Diffusion Coefficient of Benzoic Acid in Various Concentrations of Polymeric Solutions at 25°

Viscosity-Enhancing Agent	Percent	Solubility, mg/ml	Density, g/ml	η_{rel}[a]	$10^5 D_{expt}$, cm²/sec
Methylcellulose	0.1	3.25	0.9976	1.47	1.036
	0.3	3.26	0.9979	3.65	0.678
	0.5	3.32	0.9983	8.07	0.298
	0.6	3.31	0.9985	12.90	0.240
Hydroxypropyl cellulose	0.1	3.32	0.9978	4.71	0.650
	0.2	3.29	0.9979	8.71	0.372
	0.3	3.30	0.9981	14.19	0.186
Guar gum	0.1	2.96	0.9975	3.30	1.055
	0.2	3.18	0.9982	9.31	0.446
	0.3	2.75	0.9983	25.86	0.167
Xanthan gum	0.025	—	0.9977	2.53	—
	0.05	3.17	0.9977	3.83	0.787
	0.1	3.18	0.9984	8.07	0.284
	0.15	3.10	0.9985	15.72	0.101

[a] Capillary method.

The influence of viscosity of polymeric solutions on the dissolution rate of soluble inorganic salts was studied (8). No one equation relating rate and bulk viscosity fitted the data. By utilizing an effective viscosity, a plot of the data was approximated by a single curve, which was represented by an empirical equation.

There appears to be no general expression relating the dissolution rate to viscosity. Assuming that, with various solutes and polymeric solutions of markedly different ionic and chemical nature, factors other than viscosity act and affect the dissolution rate at a given viscosity, three nonionic carbohydrate polymers were studied with the thought that the interactions would be essentially constant and that the relation of dissolution rate to viscosity could be better expressed.

EXPERIMENTAL

Dissolution Rate Determinations—The procedure for tablet production and the dissolution apparatus were similar to those previously described (9). Spherical 1.273 ± 0.005-cm tablets of pure benzoic acid were compressed at 2270 kg of force by a hydraulic press[1]. All determinations were made in triplicate at 25 ± 0.1° and at a stirring speed of 324 rpm. The 2 liters of dissolution medium was changed at appropriate intervals so that the concentration of dissolved benzoic acid was not permitted to exceed 3% of its solubility. With each change of dissolution medium, the sphere was weighed and its diameter was measured with a micrometer. Solutions were prepared by a conventional method and allowed to stand 24 hr before use as the dissolution media. Dissolution rates were determined in various concentrations of aqueous methylcellulose[2], hydroxypropyl cellulose[3], xanthan gum[4], and guar gum[5] solutions.

Other Parameters—The solubilities of benzoic acid in various concentrations of polymeric solutions as given in Table I were determined as reported earlier (9). The densities of the solutions were measured using a pycnometer. Viscosities were measured by using a capillary[6] and a rotational[7] viscometer. The diffusion coefficients were determined by use of a diffusion cell previously described (10). The value in Table I is an average of three determinations for each concentration.

RESULTS AND DISCUSSION

Bulk Viscosity—For the concentrations observed, the addition of methylcellulose, hydroxypropyl cellulose, guar gum, and xanthan gum in solution increases the viscosity by at least 15-fold as shown in Fig. 1. The addition of these polymer molecules in solution decreases to less than one-half the dissolution rate of benzoic acid as shown in Fig. 2. The solubility of benzoic acid in water is not significantly affected by the presence of any of these polymers as shown in Table I.

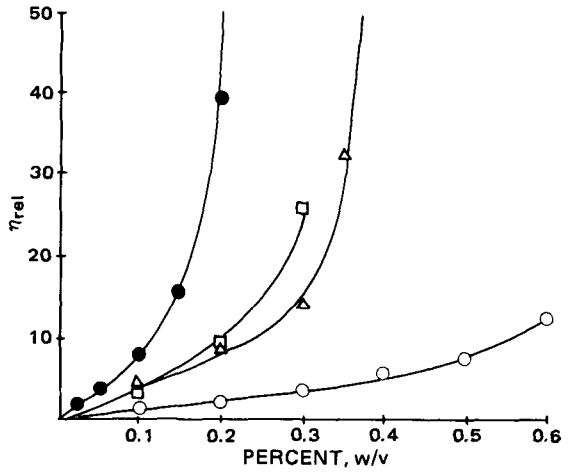

Figure 1—*Relative viscosity (η_{rel}) as a function of concentration in water at 25°. Key: (○) methylcellulose; (△) hydroxypropyl cellulose; (□) guar gum; and (●) xanthan gum.*

With no significant change in solubility, the only experimental variable affecting the dissolution rate appeared to be viscosity. Thus, one would anticipate that at a given viscosity of the dissolution medium, the dissolution rate of benzoic acid would be the same regardless of the noninteracting dissolution medium.

Figure 3 shows the relation of the dissolution rate and relative viscosity as determined by a capillary viscometer. It does not appear that one equation will relate the dissolution rate and bulk viscosity. Since the viscosity measured by the capillary method is a single shear rate viscosity, it probably does not represent the actual viscosity in the dissolution environment.

The viscosity-enhancing polymers studied form pseudoplastic solutions, which possess viscosities that vary with shear rate. The viscosities of the polymeric solutions were measured at rotational speeds from 0.3 to 60 rpm. Similar to the example of the methylcellulose solutions shown in Fig. 4, all of the polymeric solutions exhibited pseudoplastic flow at low rotational speed (<10 rpm), but at speeds >10 rpm, the viscosity did not decrease as the shear rate was increased. The constant viscosity at high shear has been called the upper Newtonian viscosity for dilute so-

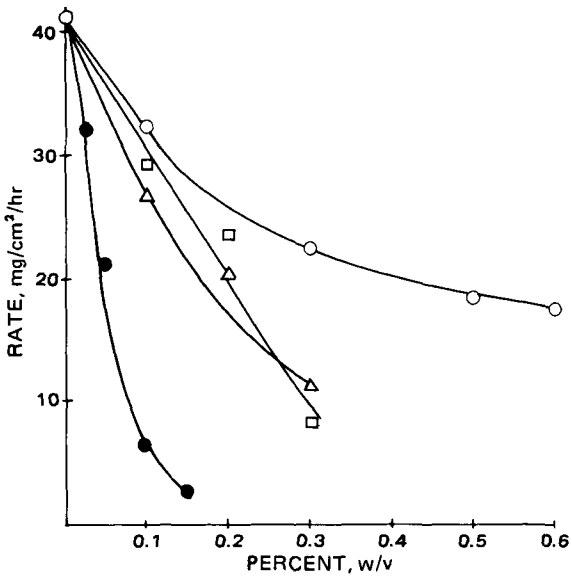

Figure 2—*Dissolution rates of benzoic acid in various concentrations of aqueous polymeric solutions. Key: (○) methylcellulose; (△) hydroxypropyl cellulose; (□) guar gum; and (●) xanthan gum.*

[1] Carver press, model C, Fred S. Carver, Inc.
[2] USP, type 1500 cp, City Chemical Corp.
[3] Klucel, grade HF, Hercules Inc.
[4] Kelzan, Kelco Division of Merck & Co., Inc.
[5] Colony Impt. & Expt. Corp.
[6] Ostwald-Fenske.
[7] Brookfield model LVT Synchro-lectric, Brookfield Engineering Lab.

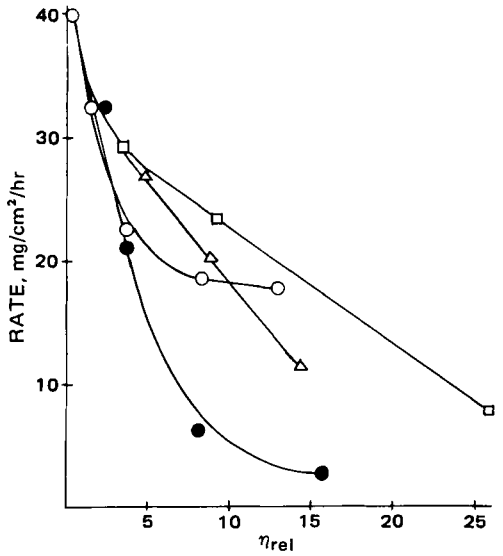

Figure 3—*Influence of relative viscosity of various polymeric solutions on dissolution rates of benzoic acid at 25°. Key: (○) methylcellulose; (△) hydroxypropyl cellulose; (□) guar gum; and (●) xanthan gum.*

lutions (11). At high shear rates, dissolved polymer chains are wholly disentangled and aligned in the direction of flow. As there is no remaining structure to be broken by further increases in shear rate, the viscosity reaches a constant value. In the viscometer at 60 rpm, the shear rate is ~200 sec^{-1} (12). The viscosity determined at speeds >10 rpm should represent the bulk viscosity in the dissolution apparatus (in which the 324 rpm provided a shear rate >200 sec^{-1}) better than the capillary viscosity.

The influence of viscosity measured at 1.5 rpm on the dissolution rate of benzoic acid at 25° in aqueous methylcellulose, hydroxypropyl cellulose, guar gum, and xanthan gum solutions is shown in Fig. 5. For the nonionic polymers (methylcellulose, hydroxypropyl cellulose, and guar gum) the dissolution rate is decreased rapidly to almost the same extent. At rotational speeds >10 rpm, the experimental values of dissolution rate and viscosity of solutions of methylcellulose, hydroxypropyl cellulose, and guar gum essentially fall on a single curve (Fig. 6) indicating that for a dissolution medium of similar ionic and chemical nature, there is a correlation between dissolution rate and viscosity.

Microviscosity—The dilemma with polymeric solutions is to express an observed viscosity, which is a true reflection of the impedance to molecular transport in solution. Since in solutions of macromolecules the bulk viscosity as measured by a viscometer does not necessarily represent the viscosity through which the solute molecules travel, a viscosity measured without the mechanical influence of a viscometer was considered. In the Stokes-Einstein equation, there is an inverse relationship between the viscosity and the diffusion coefficient. Thus, an attempt was made to relate the diffusivity of benzoic acid in the polymeric solution to viscosity by use of the Stokes-Einstein equation, as the concentration of benzoic acid was dilute and the radius (2.95 Å) of the benzoic acid molecule is smaller than that of the solvent molecule (13). The viscosity

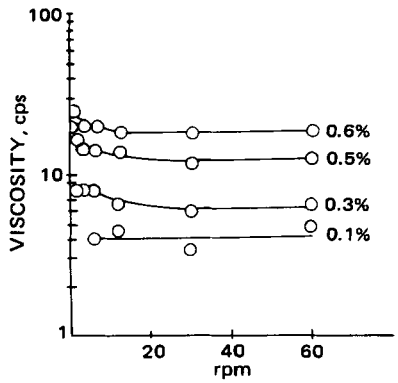

Figure 4—*Influence of rotations per minute on viscosities of aqueous solutions of various concentrations of methylcellulose.*

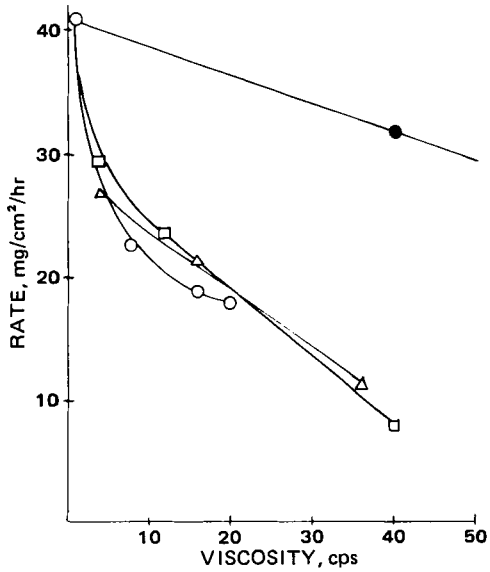

Figure 5—*Influence of viscosity at 1.5 rpm on the dissolution rate of benzoic acid in aqueous polymeric solutions. Key: (○) methylcellulose; (△) hydroxypropyl cellulose; (□) guar gum; and (●) xanthan gum.*

(η_D) of the microenvironment was calculated using the experimental diffusion coefficients (D_{expt}) in various concentrations of polymeric solutions by:

$$\eta_D = \frac{kT}{6\P rD_{expt}} \qquad \text{(Eq. 1)}$$

where k is the Boltzmann constant, T is the absolute temperature, and r is the radius of the benzoic acid molecule. For example, with benzoic acid dissolving in 0.1% methylcellulose solution at 25°, the D_{expt} is 1.036 × 10^{-5} cm^2/sec, and:

$$\eta_D = \frac{(1.38066 \times 10^{-16})(298)}{6\P\,(1.036 \times 10^{-5})(1.95 \times 10^{-8})}$$
$$= 0.0071 \text{ poise}$$

According to a previous report (14), the D_{expt} in polymeric solutions may be corrected for the obstructive effect of the polymer chains by the relation:

$$D_{true} = \frac{D_{expt}}{(1 - 1.5\,\phi)} \qquad \text{(Eq. 2)}$$

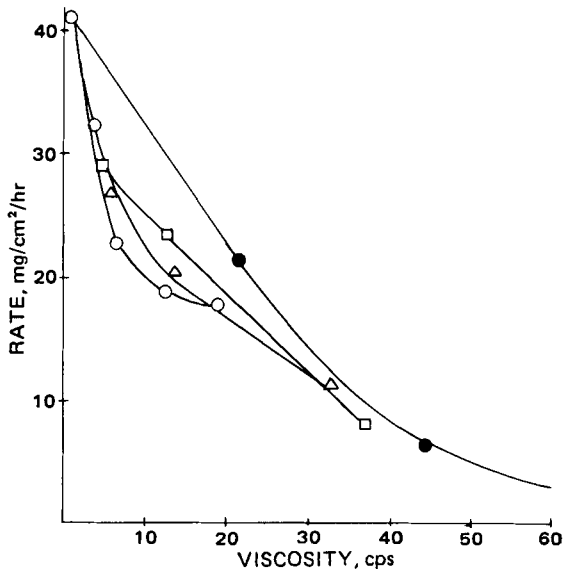

Figure 6—*Influence of viscosity at 60 rpm on dissolution rate of benzoic acid in aqueous polymeric solutions. Key: (○) methylcellulose; (△) hydroxypropyl cellulose; (□) guar gum; and (●) xanthan gum.*

Table II—Dissolution Rate of Benzoic Acid in Various Concentrations and Viscosities of Polymeric Solutions at 25°

Viscosity-Enhancing Agents	Percent	η_D, cps[a]	$f(\eta)$[b]	R, mg/cm²/hr	$\frac{R_{calc}}{R}$[c]
Methylcellulose	0.1	0.71	0.864	32.41	1.00
	0.3	1.09	0.925	22.79	1.20
	0.5	2.48	1.707	18.82	0.99
	0.6	3.08	1.848	16.36	0.96
Hydroxypropyl cellulose	0.1	1.14	1.117	26.79	0.99
	0.2	1.99	1.500	20.39	1.03
	0.3	3.98	1.704	11.66	1.00
Guar gum	0.1	0.70	0.841	29.26	1.02
	0.2	1.66	1.487	23.51	0.95
	0.3	4.43	1.592	8.15	1.01
Xanthan gum	0.025	—	—	32.11	—
	0.05	0.94	—	21.33	—
	0.10	2.60	—	6.55	—
	0.15	7.33	—	2.91	—

[a] Calculated by Eq. 1. [b] Calculated by Eq. 5. [c] Calculated by Eq. 7.

where ϕ is the volume fraction of the polymer. The volume fraction can be calculated from the concentration of the solution using the partial specific volume obtained by density measurements. The partial specific volume of each type of polymeric solution was evaluated by a plot of density against concentration according to the relationship:

$$\rho = \rho_{H_2O} + (1 - V\rho_{H_2O})C \qquad \text{(Eq. 3)}$$

where ρ and ρ_{H_2O} are the densities of the solution and the solvent, respectively, C is the concentration, and V is the partial specific volume. The volume fraction of the polymer was calculated from the partial specific volume and used in Eq. 2 to calculate D_{true}. In none of the systems studied did the difference between the D_{true} and D_{expt} exceed 0.3%.

The viscosity calculated by Eq. 1 and the dissolution rate are given in Table II. As seen in Fig. 7, as the viscosity of the dissolution media is increased, the dissolution rates are slowed to approximately the same extent. A single curve could be constructed to fit the experimental values.

Relation of Dissolution Rate and Viscosity—When the dissolution of a one-component, nondisintegrating sphere occurring in a nonreactive medium at sink conditions is diffusion controlled, the dissolution rate (R) may be expressed as (9):

$$R = \frac{DC_s}{h} \qquad \text{(Eq. 4)}$$

where D is the diffusion coefficient of the solute molecule, h is the effective film thickness, and C_s is the solubility. The experimental conditions used in determining the dissolution rate suggest that the diffusion layer model is operative (10). As shown in Fig. 8 there is a linear relationship between D_{expt} and $1/\eta_D$. It has been shown that at a fixed bulk viscosity the dissolution rate is not a linear function of D_{expt} (10). Similarly, as shown in Fig. 8, the relationship between dissolution rate of benzoic acid and D_{expt} in polymeric solutions is nonlinear. As the relationships of dissolution rate to viscosity and diffusion coefficient are curvilinear, a viscosity function $f(\eta)$ was introduced into Eq. 4:

$$R = \frac{DC_s}{h} f(\eta) \qquad \text{(Eq. 5)}$$

Experimentally all terms were evaluated so that the viscosity function could be calculated, assuming that h remained constant. For example, the viscosity function for 0.1% methylcellulose solution at 25° is:

$$f(\eta) = \frac{32.42 \times 32.2 \times 10^{-4}}{1.036 \times 10^{-5} \times 3600 \times 3.25} = 0.864$$

The values of the viscosity function for various polymeric solutions are given in Table II.

The relationship of the viscosity function to the η_D is shown in Fig. 9, and the equation for this relationship in these nonionic polymeric solu-

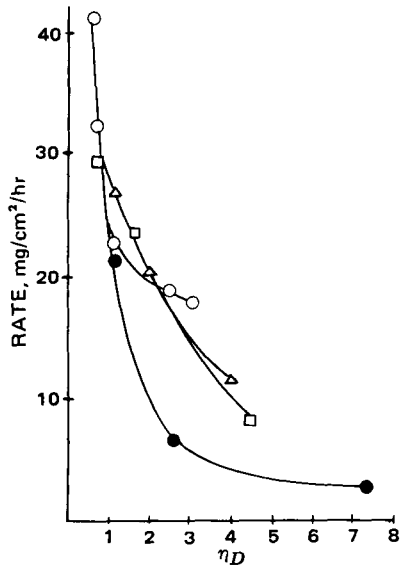

Figure 7—*Influence of η_D on dissolution rate of benzoic acid in aqueous polymeric solutions. Key: (○) methylcellulose; (△) hydroxypropyl cellulose; (□) guar gum; and (●) xanthan gum.*

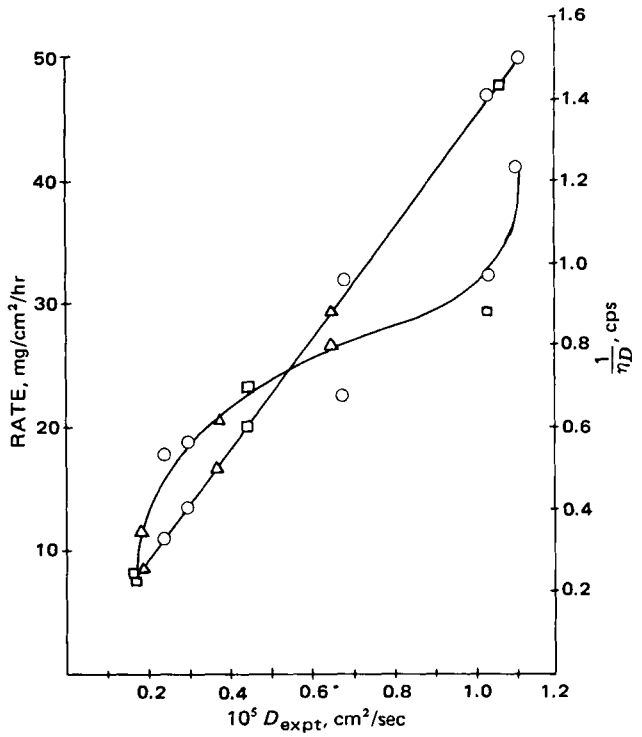

Figure 8—*Relationship of D_{expt} to $1/\eta_D$ and dissolution rate for aqueous polymeric solutions. Key: (○) methylcellulose; (△) hydroxypropyl cellulose; and (□) guar gum.*

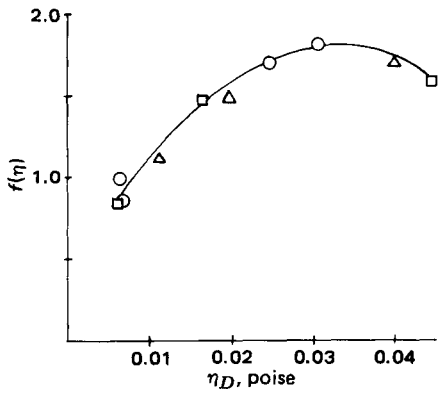

Figure 9—*Relation of η_D to viscosity function. Key: (○) methylcellulose; (△) hydroxypropyl cellulose; and (□) guar gum.*

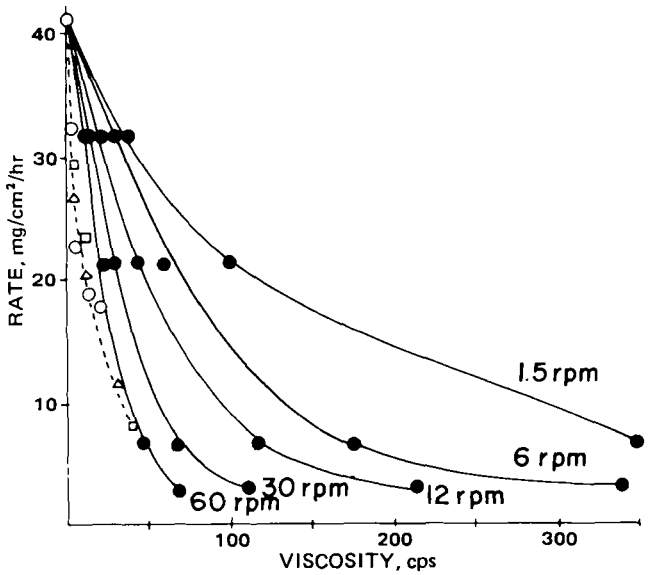

Figure 10—*Influence of rotations per minute on viscosity and dissolution rate in various polymeric solutions. Broken curve is a composite for solutions of nonionic polymers. Key: (○) methylcellulose; (△) hydroxypropyl cellulose; (□) guar gum; and (●) xanthan gum.*

tions is:

$$f(\eta) = 0.295 + 89.9\eta_D - 1360\eta_D^2 \qquad \text{(Eq. 6)}$$

Determination of η_D of a solution permits the calculation of the viscosity function, which is then used in Eq. 7 to calculate the dissolution rate. For example, in a 0.1% methylcellulose solution at 25° the η_D is 0.0071 poise, and the viscosity function is:

$$f(0.0071) = 0.295 + (89.9 \times 0.0071) - (1360 \times 0.0071^2)$$
$$= 0.865$$

Thus, the dissolution rate of benzoic acid in solutions of carbohydrate polymers of similar chemical and nonionic nature may be expressed as:

$$R = \frac{DC_s}{h}(0.295 + 89.9\eta_D - 1360\eta_D^2) \qquad \text{(Eq. 7)}$$

where D and C_s are the diffusion coefficient and solubility in the dissolution medium, respectively, possessing a microviscosity of η_D poises. The dissolution rate calculated by use of Eq. 7 and the experimental dissolution rates are compared in Table II.

Influence of Ionization of Polymer—Xanthan gum, which is chemically similar to the viscosity-enhancing polymers studied and is anionic, was selected to demonstrate the influence of electrical interactions on dissolution. In Figs. 1–3 the relations of concentration, relative viscosity, and dissolution rates are shown for xanthan gum. The influence of xanthan gum is more marked than the nonionic polymers. In Figs. 3 and 5 the rate–viscosity curve in solutions of the xanthan gum does not appear to have the same relationship as in solutions of the nonionic polymers.

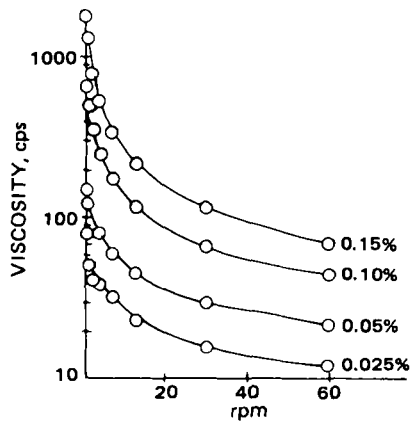

Figure 11—*Influence of rotations per minute on viscosity of solutions of various concentrations of xanthan gum.*

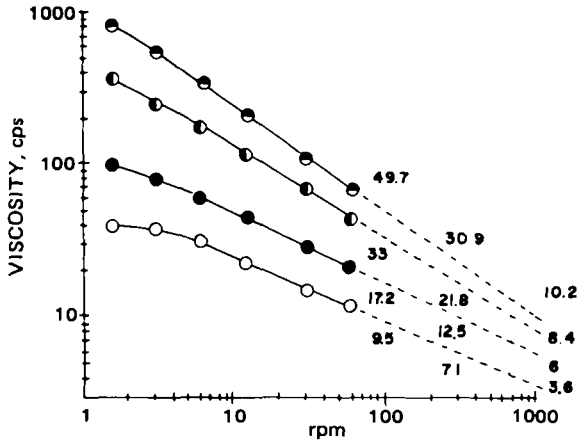

Figure 12—*Log–log relationship of viscosity and rotations per minute for solutions of xanthan gum. The viscosities at 100, 200, and 1000 rpm are given in the figure. Key: (○) 0.025%; (●) 0.05%; (◐) 0.1%; and (⊖) 0.15%.*

As the shear rate is increased by faster speeds of the rotational viscometer, the rate–viscosity curve in solutions of xanthan gum moves downward approaching the curve in solutions of the nonionic polymers, as shown in Fig. 10. Thus, the solutions of xanthan gum are pseudoplastic, but a shear rate greater than that provided by the rotational viscometer is required to reach the upper Newtonian viscosity, as shown in Fig. 11. The viscosity measured at 60 rpm does not represent the bulk viscosity of the solution of xanthan gum in the dissolution apparatus. To estimate the viscosity of the solution of xanthan gum at greater shear rates, the logarithm of viscosity was plotted against the logarithm (rpm) for the various concentrations of xanthan gum. The linear portions of the curves were extrapolated to estimate the viscosities at 100, 200, and 1000 rpm, as shown in Fig. 12.

In Fig. 13 the dissolution rates of benzoic acid are plotted as a function of the extrapolated viscosities at 100, 200, and 1000 rpm. The relationship of dissolution rate to viscosity in solutions of xanthan gum is not the same as that for the solutions of the nonionic polymeric solutions studied. Although the chemical nature is similar for all the polymers, the xanthan gum is anionic. Thus, the transport of benzoic acid in solutions of xanthan gum is complicated by the electrical charge on the xanthan gum chain.

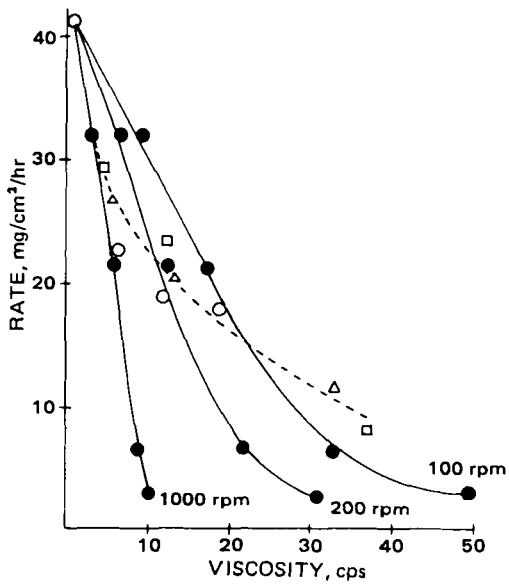

Figure 13—*Influence of viscosity at 100, 200, and 1000 rpm on dissolution rate of benzoic acid in aqueous solutions of xanthan gum. Broken curve is a composite for solutions of nonionic polymers. Key: (○) methylcellulose; (△) hydroxypropyl cellulose; (□) guar gum; and (●) xanthan gum.*

It was reported (15) that for ferricyanide ions diffusing in solutions of xanthan gum, the diffusion coefficient was decreased as much as 20-fold and was decreased as the shear rate was increased. It is thought that the shear causes the xanthan gum molecule to extend, exposing charge sites, and then the interaction between the solute and the charge sites changes diffusivity.

In addition, the viscosity measured by the viscometer may not represent the actual resistance to solute molecule transport. The values of the η_D of solutions of xanthan gum were calculated by Eq. 1. The relation of dissolution rate to viscosity of solutions of xanthan gum shown in Fig. 7 is not the same as the relation of dissolution rate to viscosity of solutions of the nonionic polymers. The difference may be caused by the interaction between the benzoic acid molecule and the anionic segments of the xanthan gum.

It appears that for viscosity-enhancing polymers of similar chemical and nonionic nature, a relationship may be expressed between the viscosity of the dissolution medium and the dissolution rate of a solid. However, if the chemical or ionic nature of the polymers is different, additional factors that influence dissolution rate are introduced and must be considered.

REFERENCES

(1) E. Roehl, C. V. King, and S. Kipness, *J. Am. Chem. Soc.*, **61**, 2290 (1939).

(2) T. Kressman and J. Kitchener, *Discuss. Faraday Soc.*, **7**, 90 (1949).

(3) C. V. King and M. M. Braverman, *J. Am. Chem. Soc.*, **54**, 1744 (1932).

(4) R. J. Braun and E. L. Parrott, *J. Pharm. Sci.*, **61**, 175 (1972).

(5) P. Roller, *J. Phys. Chem.*, **39**, 221 (1935).

(6) A. P. Colburn, *Trans. Inst. Chem. Eng.*, **29**, 174 (1949).

(7) C. Wagner, *J. Phys. Chem.*, **53**, 1030 (1949).

(8) A. T. Florence, P. H. Elworthy, and A. Rahman, *J. Pharm. Pharmacol.*, **25**, 779 (1973).

(9) E. L. Parrott and V. K. Sharma, *J. Pharm. Sci.*, **56**, 1341 (1967).

(10) R. J. Braun and E. L. Parrott, *ibid.*, **61**, 592 (1972).

(11) H. Schott, "Remington's Pharmaceutical Sciences," 15th ed., Mack Publishing, Easton, Pa., 1975, pp. 350–367.

(12) "Brookfield Model LVT Operating Instructions," Brookfield Engineering Laboratories, Stoughton, Mass., 1980.

(13) J. T. Edward, *J. Chem. Ed.*, **47**, 261 (1970).

(14) M. Lauffer, *Biophys. J.*, **1**, 205 (1961).

(15) D. W. Hubbard, F. D. Williams, and G. P. Heinrich, in "Proceedings of the International Congress on Rheology," 8th ed., G. Astarita, G. Marrucci, and L. Nicolais, Eds., Plenum, New York, N.Y., 1980, pp. 319–324.

ACKNOWLEDGMENTS

Abstracted in part from a dissertation submitted by N. Sarisuta to the Graduate College, University of Iowa, in partial fulfillment of the Doctor of Philosophy degree requirements.

Synthesis and Catalytic Activity of Poly-L-Histidyl-L-Aspartyl-L-Seryl-Glycine

A. N. SARWAL, E. O. ADIGUN, R. A. STEPHANI, and A. KAPOOR ×

Received July 21, 1981, from the *College of Pharmacy and Allied Health Professions, St. John's University, Jamaica, NY 11439.* Accepted for publication February 1, 1982.

Abstract □ Poly(His-Asp-Ser-Gly) was synthesized from the fully protected tetrapeptide active ester hydrochloride, which was prepared by stepwise coupling, using pentachlorophenyl ester and mixed anhydride methods. Complete deprotection of the protected tetrapeptide polymer was achieved by using 90% trifluoroacetic acid. The free polymer was dialyzed for 24 hr using a membrane (which retains molecules with molecular weights >5000). The catalytic activity was determined by studying the hydrolysis of *p*-nitrophenyl acetate in 0.2 *M* phosphate buffer (pH 7.4) at 37°. The catalytic coefficient of the dialyzed polymer was found to be 138 liters/mole/min.

Keyphrases □ Poly-L-His-L-Asp-L-Ser-Gly—synthesis and catalytic activity, polymer, pentachlorophenyl ester, hydrolysis □ Polymer—synthesis and catalytic activity of poly-L-His-L-Asp-L-Ser-Gly, pentachlorophenyl ester, hydrolysis □ Hydrolysis—synthesis and catalytic activity of poly-L-His-L-Asp-L-Ser-Gly, pentachlorophenyl ester, polymer

The use of poly(amino acids) as esterase models for structural and mechanistic problems of proteolytic enzymes has been very useful (1, 2). The poly(amino acids) that have been used for this purpose include homopolymers, copolymers, and sequential polypeptides. Sequential polypeptides provide one of the best means to study the factors affecting the folding of various enzymes, since they permit the placement of specific side chains at specific locations on a polypeptide backbone. Thus, suitable folding brings important side chain functionalities required for the activity into closer proximity, even though these amino acids lie at different distances in the enzyme sequences.

Considerable attention has been focused recently on the role played by L-histidine and L-serine in the active site of chymotrypsin and other proteolytic enzymes toward the hydrolysis of various esters such as *p*-nitrophenyl acetate (3, 4). Synthesis and catalytic activity of a number of peptides incorporating histidine and serine have been recently reported (5–7) as esterase models. The synthesis of the pentapeptide; L-Ser-γ-aminobutyryl-L-His-γ-aminobutyryl-L-Asp which had a catalytic coefficient of 147 liters/mole/min has been reported (5). The synthesis of a relatively more potent esterase model, L-His-Gly-L-Asp-L-Ser-L-Phe which had a catalytic coefficient of 179 liters/mole/min has also been reported (6). The comparison of the catalytic activity of various peptide esterase models led to the conclusion that peptides that incorporated L-aspartic acid in addition to L-histidine and L-serine showed considerable increase in catalytic activity (7). For example, L-His-L-Ala-L-Asp-Gly-L-Ser showed a catalytic activity of 210 liters/mole/min. The corresponding pentapeptide, L-His-L-Ala-L-Glu-Gly-L-Ser, where aspartic acid was replaced by glutamic acid, had a catalytic activity of 87

0022-3549/82/1200-1380$01.00/0